AD-A163 713 ACTA ARMAMENTARII (SELECTED ARTICLES)(U) FOREIGN TECHNOLOGY DIV WRIGHT-PATTERSON AFB OH 06 JAN 86 FTD-ID(RS)T-0913-85 1/1

UNCLASSIFIED F/G 21/8 NL

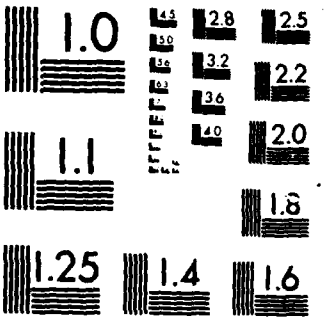

(2)

FTD-ID(RS)T-0913-85

AD-A163 713

FOREIGN TECHNOLOGY DIVISION

ACTA ARMAMENTARII

(Selected Articles)

Approved for public release;
distribution unlimited.

EDITED TRANSLATION

FTD-ID(RS)T-0913-85 6 Jan 86

ACTA ARMAMENTARII (Selected Articles)

English pages: 21

MICROFICHE NR: FTD-85-C-001342
Source: Binggong Xuebao, Nr. 3, August 1984, pp. 31-35; 61-64

Country of origin: China
Translated by: SCITRAN
F33657-84-D-0165
Requester: FTD/TQTA

PREPARED BY:

TRANSLATION DIVISION
FOREIGN TECHNOLOGY DIVISION
WP-AFB, OHIO.

Table of Contents:

GRAPHICS DISCLAIMER

All figures, graphics, tables, equations, etc. merged into this translation were extracted from the best quality copy available.

SEM Examination of Molybdenum Nozzle and Investigation of the Erosion Mechanism*

Jiang Fan and Gao Xinyi

[Abstract] Scanning Electron Microscopy (SEM) is used to examine the molybdenum nozzle of an anti-tank missile after a firing test. The erosion mechanism of the molybdenum nozzle, including the combination of factors such as plasticity-cohesiveness fluxion, mechanical abrasion, cold-hot brittle crack, eutectic melting and chemical corrosion, is investigated. It not only is determined by the physical, mechanical and chemical properties of the molybdenum nozzle material itself, but also is related to the characteristics of the propellant, wrapping coat, insulating coat and combustor. In addition, corresponding measures are introduced to alleviate erosion.

1. Introduction

Most anti-tank missles developed and deployed in the world use pure molybdenum combustor nozzles. Some of the raw material is cast molybdenum made by vacuum melting. Some is rolled or sintered by vertical melting. The raw material is machined into nozzles. Or, nozzles may be fabricated directly by using power metallurgical techniques. A great deal of static and flight experiments confirmed thata different extent of erosion occurs at 15-25 s after the combustor is ignited no matter which type of

*Manuscript received on March 24, 1983, revised on April 9, 1984.

nozzle is used. In some cases, the erosion is minor and the performance of the combustor will not be affected. In other cases, the size and shape of the nozzle are significantly changed. Local melting or washing grooves may even appear in the contracting section and the throat, leading to the serious deterioration of the combustor performance.

2. SEM Examination

In this work, three nozzles of different structures from two models of combustors were examined after combustor testing.

The molybdenum nozzle was first cut axially in order to select the portions to be examined. It was then cut into 10 x 10 mm^2 square blocks and observed under a Model ASM-SX Scanning Electron Microscope. The operating conditions are: accelerating voltage 25 KV and electron beam current 0.02μA. Secondary electron images were taken as shown in Figures 2.1~2.7.

Next, back scattered electron image and the chemical composition distribution of the black precipitate in the diffusive section of the Model A nozzle were obtained. The conditions of observation were 10 KV and 0.1μA. It was found that elemental carbon is uniformly distributed. We did not find elements such as Fe, Mo, Cr and Si.

In addition, the specimens were polished. Figure 2.8 shows a photograph of the polished Model C nozzle under an optical microscope. We can clearly see some oxide impurities. It was then etched in a boiling HF and HNO_3 solution. The photograph is shown in Figure 2.9.

It was observed that there was no apparent difference in the etched metallographic structure either at the substrate or on the surface. We did not see any transitional structure either. The crystal size in the contracting section is larger than that in the difference section, which confirms that the temperature in the contracting section has already exceeded the recrystallization temperature of molybdenum in the ignition process.

/32

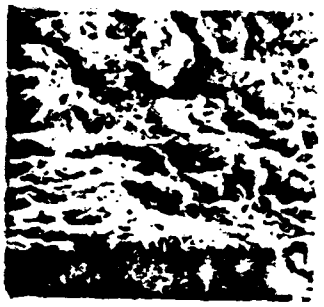

Figure 2.1 Front Proportion of Model C Diffusive Section at 21X. Special Feature: Island-shaped and stripe channels.

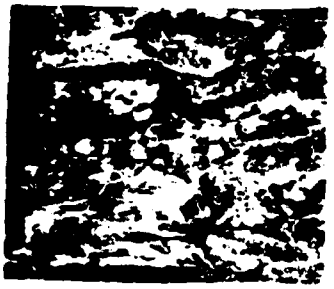

Figure 2.2 Middle Portion of Model C Diffusive Section at 21X. Special Feature: Inclined grooves.

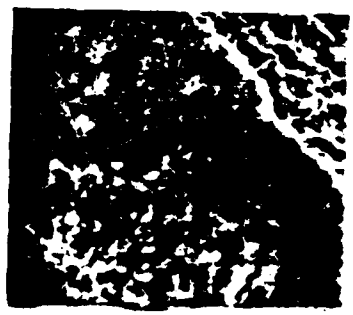

Figure 2.3 Middle Portion of Model C Diffusive Section at 350X.

Special Feature: Microcracks at 45~60° with respect to the direction of the deep groove.

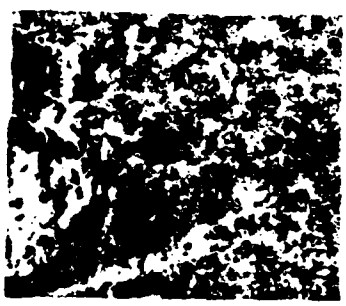

Figure 2.4 Contracting Section of Model C at 21X.

Special Feature: Deep horn-shaped channel.

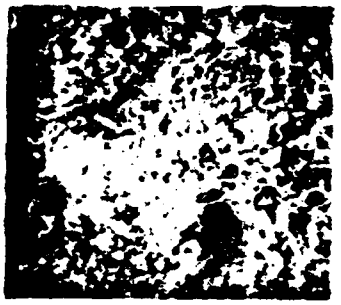

Figure 2.5 Contracting Section of Model C at 350X.

Special Feature: Visible transverse cracks at the bottom of the groove.

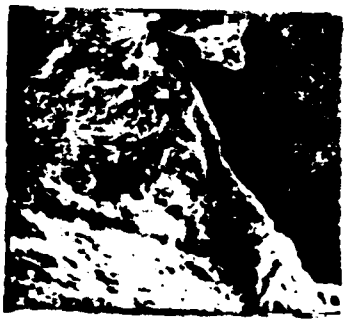

Figure 2.6 Front Portion of the Model A Contracting Section at 21X

Special Feature: Serious erosion and melting at the leading edge.

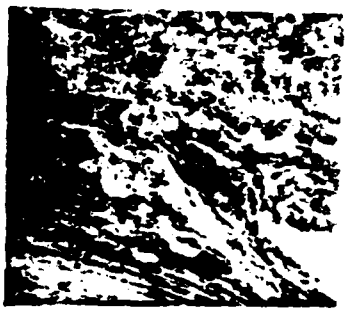

Figure 2.7 Front Portion of the Model B Contracting Section at 21X.

Special Feature: Slight erosion with scratches on the lower left.

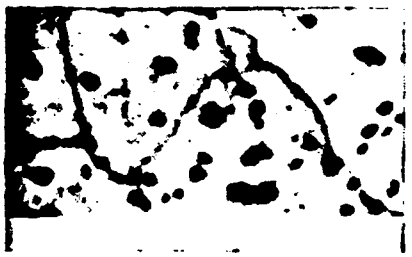

Figure 2.8 Metallographic Structure After Polishing

At a low SEM magnification (21X), all specimens show a stero/33 morphology. The channels and grooves are apparently visible. It is possible to identify the inlet contracting section and the outlet diffusive section on the picture. Some of them showed stripes or channels (such as Figures 2.1, 2.2, 2.4) and some exhibit signs of melting (such as Figure 2.6). At higher

magnifications (such as 350X), microcracks were observed in the melted graters (such as Figure 2.3). Small cracks at lower magnifications (as in Fig. 2.4) become deep channels (such as Figure 2.5). It is obvious that erosion also took place inside these channels.

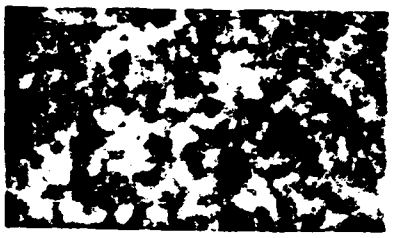

Figure 2.9 Etched Metallographic Structures

3. Investigation of Erosion Mechanism

The combustors of all the molybdenum nozzles examined used a cobalt-2 solid rocket propellant. Its combustion gas temperature is 1900-2300°C while the melting temperature of molybdenum is 2620°C. Why is it susceptible to various degrees of erosion? There are many factors involved. Our analysis shows the following major factors:

3.1 Plasticity-Cohesiveness Fluxion

Molybdenum nozzles are working at high temperature and stress. When the surface is heated to a high temperature, although it has not reached its melting point, yet the strength is lowered significantly[1], as shown in Table 3.1.

Table 3.1 Lowering Strength of Pure Molybdenum with Rising Temperature.

temperature/C°	25	871	1093	1371	1649	1927	2025
tensile strength/kg mm^{-2}	50	36.5	12.3	6.7	3.0	1.2	1.0

When molybdenum is heated to 2000°C, the strength is only 1/50 of that at room temperature. Because the inner surface of the nozzle is suddenly heated by the combustion gas to cause its temperature to rise rapidly, the temperature of the substrate in the nozzle is lower. The temperature gradient from the surface to the substrate of the nozzle will lead to a strength gradient, i.e., the strength of the substrate is higher than that of the surface layer. Therefore, the shear stress produced when the surface is under the action of the high pressure high speed combustion gas will cause the low strength surface layer to deform plastically, or even to flow in cohesiveness fluxion, along the direction of the combustion gas. This point was confirmed by SEM pictures.

Based on this we can deduce that when the combustion gas temperature is closer to the melting point of molybdenum, or the lcnger the operating period is, the higher the surface temperature is. It will be easier to lead to plastic deformation or cohesiveness fluxion under the shearing action of the combustion gas, i.e., the more severe the erosion of the nozzle becomes.

3.2 Mechanical Abrasion

The hardness of pure molybdenum at room temperature is not very high. It was measured to be HR=15~17. Its strength drops significantly at high temperatures. In addition, the hardness also drops rapidly. Therefore, mechanical abrasion is increased by the work action of the combustion gas (such as Figure 2.7).

Next, the propellant used contains oxides such as TiO_2 and CO_2O_3. Some double base propellants also include MgO or Al powder. The are capable of suppressing high frequency unstable combustion and improving the energy of the charge. The solid combustion product particles, however, will have a great mechanical abrasion effect on the surface of the nozzle.

In addition, the insulating coat contains refracting materials such as mica, Cr_2O_3, SiC, $3Al_2O_3 \cdot SiO_2$ and $Zn_3(PO_4)_2$. In some case, talc powder and TiO_2 are also added. When the organic silicone binder formulation or its synthesis is inadequate, then the strength of the carbide layer after ignition is very low. It may even peel off. The solid particles in the filler will be carried by the combustion gas to erode the surface of the nozzle.

3.3 Cold-hot Brittle Crack /34

Molybdenum is brittle at low temperatures. Its ductile-brittle transition temperature is in the 0°C-room temperature range. It is even more apparent when impurities such as oxygen exist (see Figure 2.8) or when the crystal size is large. If the powder making (or smelting) and sintering process is not

adequately controlled, the tendency for brittleness is even greater. When care is not exercised in processing and assembly, microcracks may be produced in the nozzle. It is extremely easy for the high temperature, high pressure combustion gas to penetrate those microcracks after ignition to wash and erode the cracks so that they are enlarged into channels.

Molybdenum is also brittle at high temperatures. Carbon-based impurities in the raw material and the contact with the high temperature carbon containing atmosphere will lead to the formation of brittle materials Mo_2C and MoC. On top of that, the thermal stress on the nozzle induced by the thermal shock during ignition, especially in the tensile stress direction, may produce thermal cracks. The deep channels shown on the SEM pictures might be caused by the expansion of the original cracks dry erosion. Microcracks, however, might be caused by thermal stress.

3.4 Eutectic Melting

It was shown in the experiment that the top of the steel jacket of the molybdenum nozzle is easily melted when the head of the contracting section of the nozzle is designed to be thin (such as Model A in Figure 3.1). The head of the contracting section is under attack from both the inside and the outside by the combustion gas. In addition, the molten steel will form a low melting eutectic [$\alpha+\varepsilon(Fe_3Mo_2)$, 1440°C] or a peritectics [$L+\varepsilon(Fe_3Mo_2)$, 1480°C; $L+\eta(FeMo)$, 1540°C][2] with molybdenum to cause the contracting section to suffer from serious erosion (see Figure 2.6). If the nozzle is designed to have a large head

(such as Model B in Figure 3.1), then erosion can significantly be reduced (see Figure 2.7).

In addition, once the insulating coat on the surface of the steel nozzle seat is peeled or locally melted, it will form a eutectic or peritectic with molybdenum to be washed away by the combustion gas.

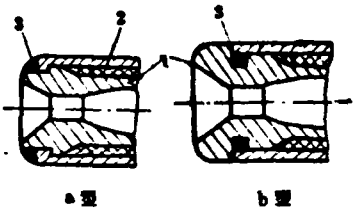

Figure 3.1 Structure of the Molybdenum Nozzle

1. nozzle
2. nozzle jacket
3. seat

3.5 Chemical Corrosion

Molybdenum is violently oxidized at temperatures above 760° C. It will form the highly volatile MoO_3. It begins to melt at above 800°C. In the pressure of nitrogen, it may form Mo_3N, Mo_2N and MoN. They will dissociate at below 1000°C[3]. During the thermal dissociation of the wrapping coat and the insulating coat and the combustion of the propellant, there will be some nitrogen and oxidizing atmosphere which will chemically corrode the molybdenum surface at high temperatures.

3.6 Other Situations

The physical and mechanical properties of the raw material of the molybdenum nozzle are different due to various methods of preparation. Therefore, its erosion resistance may also vary. Usually, the strength of deformed molybdenum is high and its sensitivity to brittleness is low. Cast molybdenum and vertical melting molybdenum come next. As for a molybdenum nozzle made by powder metallurgy, despite the use of an advanced hydraulic static pressure forming technique, the sinter density can usually reach around 97%. Its strength and hardness are lower. Therefore, its erosion resistance is relatively poor.

On the other hand, from the performance of the combustor, if a high specific thrust, high combustion velocity solid propellant is used, the combustion gas temperature is also high. Thus, nozzle erosion is naturally more serious.

In summary, factors governing the erosion of a molybdenum nozzle are not only related to the purity, structure and physical, mechanical and chemical properties of the raw material but also related to external conditions such as the composition of the propellant, wrapping coat and insulating coat and the performance of the combustor (particularly pressure and time).

4. Measures to Alleviate Erosion

(1) The binder used in the insulating coat of the combustor (such as organic silicone resin) should be modified. The strength of the carbide layer should be high to prevent peeling. The nozzle seat should have reliable protection to prevent local

melting.

(2) There should be no solid residue after the wrapping /35
coat is combusted. For instance, it is better to use polymethyl methacrylate.

(3) The contracting section of the nozzle should be designed to have a large head to avoid the jacket melting. As for the external dimensions of the nozzle, it is required that the variation at the interface should be as uniform as possible in order to minimize the concentration of stress and to avoid excessive thermal stress. The smaller the contracting section angle is, the more favorable it is to prevent the stalling and washing of solid microparticles.

(4) Deleterious impurities such as O, N and C in molybdenum should be rigorously controlled. If possible, use molybdenum containing 0.5% Ti which has better physical and mechanical properties than those of pure molybdenum. The molybdenum blank had better be processed by deformation; i.e., to roll, forge or press below its recrystallization temperature and to anneal to relieve stress in order to alter its substructure.

(5) During the processing and assembly steps, we should avoid mechanical output and tensile stress on the molybdenum nozzle in order to avoid the formation of microcracks. Because molybdenum is obviously sensitive to notch formation, if there are surface damages or microcracks on the nozzle, it is easy to lead to crack propagation during assembly or ignition.

(6) On the surface of the molybdenum nozzle, it is also possible to prepare a silicon doped molybdenum layer ($MoSi_2$) to

improve its resistance against chemical corrosion.

Finally, it must be pointed out that the range of application for molybdenum nozzles is finite. If a high energy double base charge or composite charge is chosen, molybdenum nozzles cannot do the job. It is necessary to select a more temperature resistant material such as thermally decomposed graphite, graphite precipitated tungsten or carbon/carbon composite material.

The authors wish to acknowledge that the SEM photographs in this work were taken by the Mechanical Research Institute of Anhui.

References

[1] Metallurgical Society Conferences, Refractory Metals and Alloys, Vol. 11, 1960.

[2] T.A. Kamehko, ((Principle of Metals)), Longmen United Bookstore, 1954.

[3] F.F. Khimiushin, AD-726578, 1971.

THE SEM EXAMINATION OF MOLYBDENUM NOZZLE AND THE INVESTIGATION OF EROSION MECHANISM

Jiang Fan, Gao Xinyi

Abstract

The examination has been made with SEM for the Molybdenum nozzle of the anti-tank missile after passing the firing test. The erosion mechanism of the molybdenum nozzle is investigated, including all factors such as plasticity-cohesiveness fluxion, mechanical abrasion, cold-hot brittle crack, eutectic melting, chemical corrosion, etc. It depends both on the physical, mechanical and chemical properties of the material of which the nozzle is made and on the properties of the propellant, wrapping coat, insulating coat and combustor. Measures taken for relieving erosion are correspondingly made.

EXPERIMENTAL METHOD TO MEASURE EROSIVE BURNING SPEED OF PROPELLANT USING HIGH SPEED PHOTOGRAPHY TECHNIQUE /61

Qing Ranzu

Nomenclature

A	gas flow duct cross-sectional area	A_t	cross-sectional area at nozzle throttle
b	gas flow duct width	r_0	burning speed of propellant without erosion
r	burning speed of propellant	λ	velocity coefficient of gas flow
y	burning distance of propellant	γ	ratio of specific heat
λ_e	velocity coefficient at center of window		

There are many experimental methods to study erosive burning. High speed photography through a viewing window has been widely used since the 70's [1,2]. The advantage of the method is the ability to directly, continuously measure instantaneous burning speeds of the propellant samples (including the erosive burning speed). It can also be used to study problems such as ignition as well as propagation of flames. It is considered to date a better experiental method.

1. Experimental engine configuration and measurement system

The configuration of the experimental engine with viewing window is shown in Figure 1.1. The experimental mechanism is composed of burning gas generator (gas source), experimental section and nozzle. The experimental section is mainly composed of a shell body, propellant sample and cover plate with view window. It is a rectangular configuration. Dimensions of the propellant sample are based on such variables as required gas flow characteristics, varying range of gas flow and work duration. The length should /62 not be less than 8 to 10 times the duct width. Thus, the flow characteristics of the coming flow at the view window can be guaranteed to be fully developed turbulence. This will facilitate the measuring of the burning speed under turbulent conditions.

The width of the sample is based on working time, burning speed of the sample and the required varying range of gas flow velocity for the same experiment. Under the condition of specific throttle cross-section, then, of course, the varying range of gas flow velocity depends on initial flow duct width. The viewing window is composed of one to three layers of the same or different materials. The materials for the viewing window should be highly transparent.

By changing the dimensions of the chemicals in the burning gas generator and the cross-sectional area of the throttle combined with the combustion area of the sample, the pressure at the combustion chamber and at the viewing window of the experimental section can be adjusted. A pressure-measurement hole should be drilled near the viewing window. The inner wall of the experimental section should be covered with insulating material to reduce heat losses.

The block diagram of the measurement system is shown in Figure 1.2. Major components include: pressure-recording equipment. The pressure-measurement subsystem consists of conventional pressure sensors, electricity distributing panels and oscilloscopes. It is required to measure pressures at the viewing window as well as at two to three other points. Photographs will be taken with 500 to 1000 sec^{-1} speed depending on the storage of the high speed camera and working duration. The time shown on the photo is designated as 1/1000 second. A 2600W light for news is used to illuminate the viewing window when the photos are taken. Thus clear, continuous photos can be obtained. The video-recording equipment is used to record the combustion condition. The results of the experiments can be seen throughout the progress. This will facilitate analyses, research and provide guidance for the next experimental steps.

To ensure that the engine ignition and the operation of the high speed camera are synchronous, a time control is installed

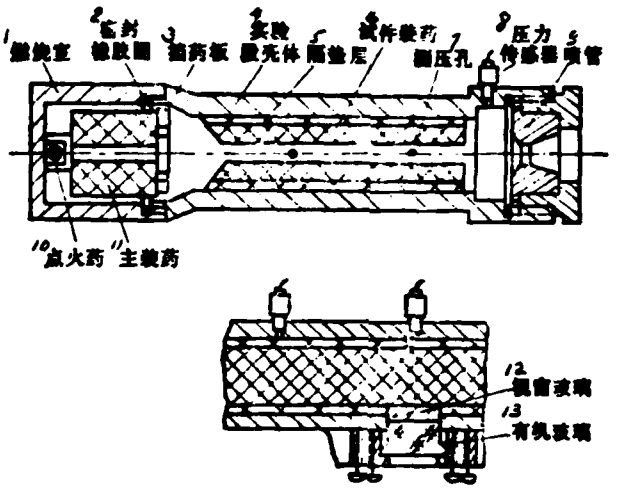

Figure 1.1 Schematic depiction of the experimental engine configuration.
1--combustion chamber; 2--sealing rubber band; 3--partition plate; 4--experimental section crust; 5--buffer layer; 6--sample chemicals; 7--pressure measurement hole; 8--pressure sensor; 9--nozzle; 10--ignition chemical; 11--major combustion chemicals; 12--viewing window glass; 13--organic glass

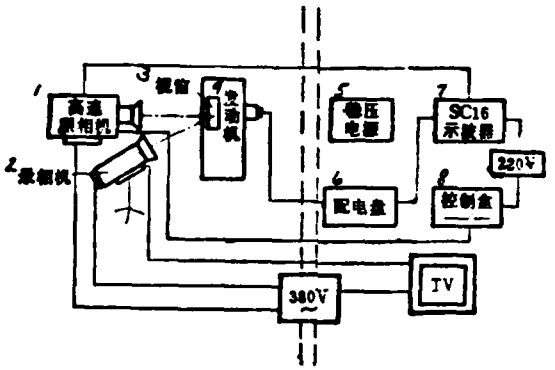

Figure 1.2 Block diagram of testing system.
1--high speed camera; 2--video recorder; 3--viewing window; 4--engine; 5--power source with regulator; 6--distribution panel; 7--SC16 oscilloscope; 8--control box

into the overall set-up. Thus, ignition is achieved in a certain amount of time after the high speed camera starts working.

In order to measure the position of the burning wave on the negative film (i.e., at the rim of the gas flow duct), also to obtain an accurate value of the duct width, microscopes can be used to study the films.

2. Basic theories of using high speed photography to measure erosive burning speed

The gas flow duct width value b at the viewing window of the experimental section can be obtained from the negative. The height of the sample is known. Therefore, the cross-sectional area A of the gas flow duct can be calculated. From the relationships of the ratio of throttle to duct, J, and velocity coefficient λ, we have

$$J = \frac{A_t}{A} = \left(\frac{\gamma+1}{2}\right)^{1/(\gamma-1)} \lambda_L \left(1 - \frac{\gamma-1}{\gamma+1}\lambda_L\right)^{1/(\gamma-1)} \qquad (2.1)$$

From equation (2.1), one can calculate the velocity coefficient λ_{LO} at the exit of the sample. The next equation is employed to calculate the velocity coefficient λ_e at the viewing window:

$$\lambda_e = \lambda_L - \Delta\lambda = \lambda_L - \frac{\Delta A_t}{A} r \rho_0 \frac{\sqrt{RT_0}}{p}\left[1 - \frac{\gamma-1}{\gamma+1}\lambda_L\right]\left[\frac{2\gamma g}{\gamma+1}\right]^{-1/2} \qquad (2.2)$$

where ΔA_b is the combustion area from the center of the viewing window to the exit of the duct, r is the sample burning speed at the viewing window.

Based on the combustion interface on the negative, one can find the gas flow duct width b(t). Calculate the duct cross-sectional area A(t). Combine with the r(t), p(t) that are actually measured. Use equation (2.2) to calculate λ_e. From the value of b, it is very easy to obtain the sample burning distance y

$$y = b - b_0 \quad \text{(single-side sample)} \qquad (2.3)$$

$$y = (b - b_0)/2 \quad \text{(double-side sample)} \qquad (2.4)$$

Find the derivative with time, then

$$r = \frac{dy}{dt} = \frac{db}{dt} \tag{2.5}$$

$$r = \left(\frac{db}{dt}\right) / 2 \tag{2.6}$$

Combine the $\lambda_e(t)$ value calculated through equation (2.2) and pressure value p(t) actually measured (using the installation condition control, the basic pressure throughout the working process is unchanged; it can generally be treated as a constant), then the burning speed relationship under constant pressure p_1 can be derived. /63

$$r = r_1(\lambda) \tag{2.7}$$

Generally, there is

$$r = r_i(\lambda) \tag{2.8}$$

That is

$$r = f(\lambda, p) \tag{2.9}$$

When r is basically unchanged, it can be considered that no more erosive effect exists and using r_o as the reference burning speed we get

$$\frac{r}{r_o} = \Phi(\lambda, p) \tag{2.10}$$

3. Typical experimental results and curve treatment

Actually measured pressure (at viewing window)--time curve is shown in Figure 3.1. Partial scope of the high speed photograph is shown in Figure 3.2. The two continuous pictures in Figure 3.2 show the situations of the initial and middle phases of the combustion. The white ranges in the pictures represent the gas flow duct, while outside of the whites represents the unburned propellant sample. The position variation of the burning interface can be clearly seen from the picture.

The microscope is used to measure the changes of gas flow duct width with time on the negatives. From equations (2.3) or (2.4) one can then obtain the relationships between the variation of burning distances and time. A representative y = y(t) curve

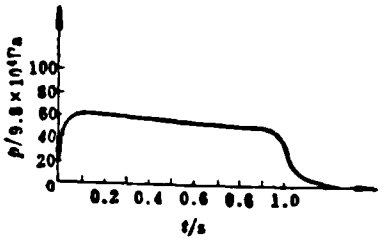

Figure 3.1. p-t curve from actual measurement

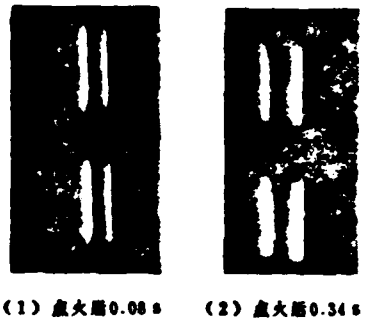

(1) 点火后0.08 s (2) 点火后0.34 s

Figure 3.2. Sample of photos taken at high speed
(1) 0.8 sec after ignition
(2) 0.34 sec after ignition

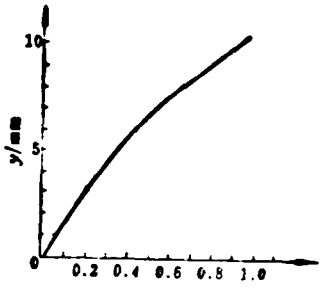

Figure 3.3. y-t curve

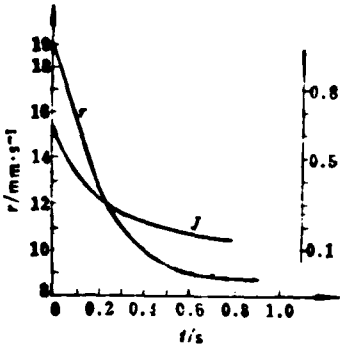

Figure 3.4. r-t, J-t curves

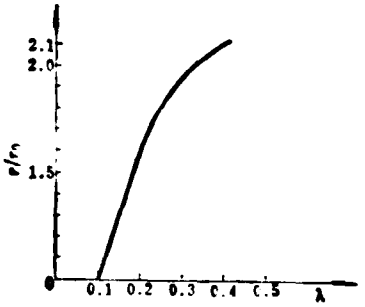

Figure 3.5 $\frac{r}{r_o}$ - λ curve

is shown in Figure 3.3. If the regression analysis method is used, the y(t) curve can be approximated by the fourth power polynomial. The typical equation is

$$y = 19.3066\,t - 23.375\,t^2 + 23.4166\,t^3 - 8.6834\,t^4 \qquad (3.1)$$

Taking the derivative of the equation, then

$$r = \frac{dy}{dt} = 19.3066 - 46.749\,t + 70.25\,t^2 - 34.733\,t^3 \qquad (3.2)$$

The functional relationship of r(t) is plotted as shown in Figure 3.4. Based upon actually measured duct width, the corresponding throttle-duct ratio J(t) can be calculated. It is also shown in Figure 3.4. The limiting point of erosion is shown on the figure. Based on it, one can calculate the erosion rate $\frac{r}{r_0}(t)$. Then, with equation (2.2), calculate $\lambda_e(t)$. The change of erosion /64 ratio with velocity coefficient can thus be found under the

condition of constant pressure (see Figure 3.5). In fact, to deal with functional relationships of the erosion ratio under specific conditions, it is not necessary to find its relations with velocity coefficients. It can be a function of closed flow or other physical quantities.

4. Conclusions

According to the results of numerous experiments, it has been found that using a high speed photography method to measure erosive burning speed of the propellant is reliable. With one experiment, one can acquire more data. The real situation of burning process can also be continuously reflected.

Lien-Tsen Wu, Ying-Hua Wei, Cheng-Hann, Tso-Lin Gao, Kwei-Ger Jian, Hsin-Hua Wang, Shou-Fan Wang, Ron-Kwei Chu and Poo Chen all participated in this work. This paper is written by Shou-Fen Wang. Poo Chen dealt with the typical curves.

REFERENCES

[1] M. K. King. Analytical and Experimental Study of the Erosive Burning of Composite Propellants, AD/A-05033, 1977

[2] M. K. Razdon, K. K. Kuo. "Measurements and Model Validation for Composite Propellant Burning under Cross Flow of Gases," AIAA J. Vol. 18, no. 6, 1980

END

FILMED

3-86

DTIC